

Countermeasure against Detector Blinding Attack with Secret Key Leakage Estimation

Dmitry M. Melkonian,^{1,*} Daniil S. Bulavkin,^{1,†} Kirill E. Bugai,¹ Kirill A. Balygin,² and Dmitriy A. Dvoretzkiy¹

¹*SFB Laboratory, Ltd, 127273 Moscow, Russia*

²*Lomonosov Moscow State University, 119991 Moscow, Russia*

(Dated: June 10, 2025)

We present a countermeasure against the detector blinding attack (DBA) utilizing statistical analysis of error and double-click events accumulated during a quantum key distribution session under randomized modulation of single-photon avalanche diode (SPAD) detection efficiencies via gate voltage manipulation. Building upon prior work demonstrating the ineffectiveness of this countermeasure against continuous-wave (CW) DBA, we extend the analysis to evaluate its performance against pulsed DBA. Our findings reveal an approximately 25 dB increase in the trigger pulse energies difference between high and low gate voltage applied under pulsed DBA conditions compared to CW DBA. This heightened difference enables a re-evaluation of the feasibility of utilizing SPAD detection probability variations as a countermeasure and makes it possible to estimate the fraction of bits compromised by an adversary during pulsed DBA.

I. INTRODUCTION

Quantum key distribution (QKD) leverages fundamental principles of quantum mechanics, notably the Wootters-Surek theorem on the impossibility of cloning a quantum state [1], to provide a theoretical framework for secure communication. This security is predicated on the inherent impossibility of perfectly replicating an unknown quantum state, thus rendering eavesdropping detectable regardless of the computational capabilities of a potential violator, often denoted as Eve. However, practical realizations of QKD systems can be vulnerable to a wide range of attacks that exploit imperfections in the employed hardware (Trojan horse [2], Laser damage [3, 4], Detector blinding [5, 6], Laser seeding [7], After-gate [8], etc [9–13]). These vulnerabilities compromise the intended security and necessitate introducing countermeasures to detect an adversary, assess and reduce its knowledge of the distributed key [14–16].

This paper continues this trend and is dedicated to improving further the methods for assessing and reducing the influence of a potential eavesdropper on distributed key, specifically the detector blinding attack (DBA). [5, 6, 17–20] for QKD systems using single photon detectors based on InGaAs/InP avalanche diodes. This type of attack aims to take control of a legitimate user's detectors to conduct a fake-state attack afterwards. Thus, DBA jeopardizes QKD systems based on "prepare and measure" protocols, which are widely used.

To address this challenge, several solely hardware-based countermeasures were introduced: monitoring the current of a single photon avalanche detector (SPAD) [21], the use of a watchdog detector [5, 22] and variable optical attenuators [23, 24], detecting weak and fast SPAD's avalanche current changes with an oscilloscope

[20]. Despite proving to be effective countermeasures against the continuous wave (CW) blinding attack monitoring the current of the SPAD, the use of the watchdog detector [25] and using variable optical attenuators failed to protect the system from the pulsed blinding attack, which remains the most challenging one among other types of bits-imposition-aimed attacks. Existing practical countermeasures against pulsed DBA typically necessitate modifications to the receiver's (Bob's) optical setup. For instance, photocurrent monitoring utilizing detector waveform analysis has effectively detected DBAs in both CW and pulsed regimes. However, the practical implementation of this approach is associated with significant complexity and cost.

Several studies have also explored the revealing of both types of DBA through the statistical analysis of detector clicks. The study by Shen et al. [26] presents an alternative countermeasure employing detector self-testing. This method utilizes an additional optical component, a quasi-single-photon source within Bob's apparatus, and its activation during randomly selected detection gates. The presence of DBA is determined by analyzing detector counts corresponding to these activation periods. A particularly promising approach involves the variation of the single-photon detector's detection efficiency [27, 28]. This countermeasure offers implementation in higher-frequency systems compared to variable optical attenuators and does not require supplementary optical components. The underlying principle of this method is to create some additional lack of information for a potential adversary about the receiver's system to make Eve leave "fingerprints" when imposing clicks. A. Huang et al. [29] tested the implementation of this countermeasure by varying the SPADs' bias voltage values and suppressing the detector's gate while conducting CW DBA. They claimed that if an adversary applies a trigger pulse within the gate instead of sending it slightly after it, the countermeasure developed by ID Quantique is vulnerable to such an attack. According to the authors, Eve

* Contact author: dmitry.melkonian@gmail.com

† Contact author: daniel.bulavkin@gmail.com

can manipulate the detector click statistic by being able to trigger detectors only at a higher supply voltage level set or by causing no clicks in case of Eve and Bob bases mismatch, regardless of supply voltage applied.

All the countermeasures mentioned above operate as attack notification systems only, meaning that if the eavesdropper's presence is detected, the whole distributed key should be discarded. The "prepare and measure" QKD protocol offered by S.N. Molotkov [30] combined with the receiver's measurement system modification [31] can theoretically still ensure a successful detection of DBA conducted and an assessment of the fraction of bits imposed by Eve. However, the practical implementation of this countermeasure presents significant challenges and requires the specific QKD protocol to be applied. ID Quantique [32, 33] also designed a multi-pixel superconducting nanowire single-photon detector, which was tested and proved its efficiency for countering DBA. The detector's click statistic analysis also allows for assessing the fraction of imposed bits. Nevertheless, most modern commercially available QKD systems still use common SPADs.

Aiming at finding a simple, easily implementable (no extra Bob's optical setup changes required), yet effective solution, we represent another detector-clicks-statistic-based approach and show that it can be used as an effective countermeasure against the pulsed DBA.

The considered approach develops an idea of randomizing the receiver's side detection probabilities via supply voltage change [27, 28], in particular, the gate voltage value variation. Although the original approach can be used neither to detect nor to assess an eavesdropper influence of the distributed key, we claim, that negative phenomenon of Eve's capability to impose a click due to distinguishability between trigger pulse energies for higher and lower supply voltage level applied can be used in favor of legitimate users to assess the number of imposed bits under pulsed DBA. In particular, we have measured the trigger pulse energies corresponding to the high and low gate voltages, revealing a substantial energy differential of approximately 25 dB under the pulsed illumination DBA. Thus, we leverage the observed significant difference between the minimum trigger pulse energy, always causing detector clicks under higher supply voltage applied, and the maximum trigger pulse energy level insufficient to start causing detector clicks under a lower supply voltage set. We demonstrate on a commercially available detector that while Eve still gains control over Bob's detectors, double or error click events are inevitably caused when Eve fails to guess correctly the gate voltage level applied to Bob's SPADs and the basis chosen. These events enable us to quantify the fraction of imposed clicks based on the double and error click statistics accumulated by legitimate users during the QKD session.

II. ATTACK DESCRIPTION AND DEFENSE MAIN PRINCIPLES

To establish a comprehensive understanding before presenting our experimental findings and their implications, we first describe the DBA under consideration. Furthermore, this section elucidates the distinctions between changing SPADs' detection efficiencies via bias and gate voltage manipulation, and the differences in SPAD responses on trigger pulses injected by Eve under CW and pulsed DBAs.

The DBA under consideration proceeds as follows: Initially, an eavesdropper intercepts and measures the quantum states transmitted by the first communication participant (Alice). Subsequently, a piece of high-power optical radiation (or high-power optical pulses) is applied to Bob's avalanche photodiode. This light initially triggers an avalanche breakdown, increasing the current and afterwards sustaining some significant current level through both the illuminated SPADs and the avalanche quenching resistor R_{bias} (Figure 1).

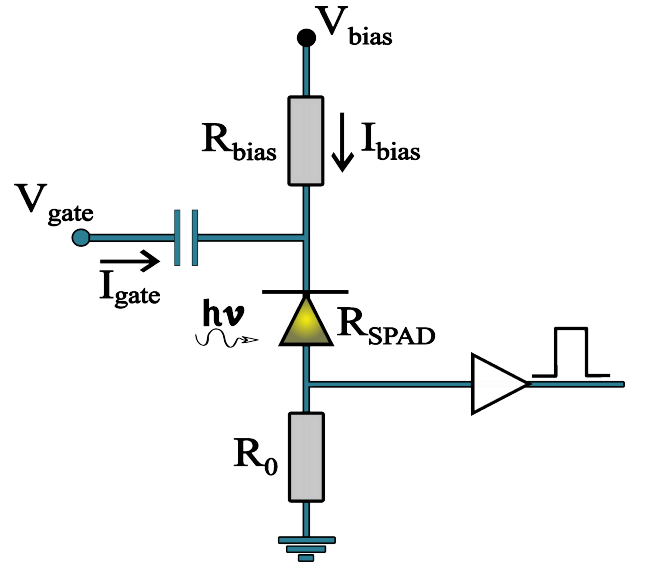


FIG. 1. Considered passive-quenching SPAD's circuit

The high current on the avalanche quenching resistor R_{bias} decreases the voltage level applied to SPAD, significantly limiting its avalanche multiplication factor (M). Therefore, the SPAD is switched from Geiger mode (where the detector is sensitive to single photons) to linear mode, becoming sensitive only to sufficiently bright pulses. The average power of the blinding optical radiation (CW DBA) or optical pulses (pulsed DBA) is selected such that it does not induce as significant a photocurrent increase (and therefore voltage drop) as an avalanche triggered by single photons in Geiger mode.

Next, Eve applies in-gate trigger pulses to Bob's detectors according to her measurement outcomes. The power of the trigger pulse is set by Eve to induce a SPAD's avalanche current (and voltage drop, respectively) that

remains below the detection threshold of the amplifier-comparator circuit when the receiver's and adversary's basis choices are mismatched. Conversely, when the bases align, the full power of the applied pulse is detected by one of the SPADs, resulting in an avalanche current sufficient to exceed the required comparator threshold. This enables the adversary to impose detector clicks without being detected while the detectors are blinded. The blinded state is maintained by either high-intensity optical pulses applied between the detector gates or continuous optical illumination.

If the SPAD's supply voltage level is lower than Eve anticipates under DBA, higher energy trigger pulses are required for successful click imposition. Thus, randomly changing the supply voltage level and monitoring the detector's click statistic, Bob forces Eve to vary trigger pulses' energy levels or time-shifts to impose clicks even during lower applied gate voltage periods. However, if the increase in trigger pulse energies is substantial enough to cause simultaneous triggering of both detectors under the default gate voltage set when Eve's and Bob's bases are mismatched, Eve would need prior knowledge of the supply voltages set at each specific detection time slot. Otherwise, an adversary would leave "fingerprints" (double and error click events) during the time slots when the high supply voltage level is applied.

Mathematically, the conditions of leaving such "fingerprints" can be expressed as:

$$2E_{always}^{high} \leq E_{never}^{low} \quad (1)$$

where E_{always}^{high} - the minimum trigger pulse energy always causing detector clicks (E_{always}) under higher supply voltage applied, E_{never}^{low} - the maximum trigger pulse energy level insufficient to start causing detector (E_{never}) clicks under lower supply voltage applied.

Several conditions must be satisfied to observe the aforementioned energy level gap increase to meet (1). First, the supply voltage level should be varied by changing the gate voltage level instead of the bias voltage level. Despite almost the same voltage difference in both cases being preserved, the gate-voltage-level-change-based approach results in a huge difference between E_{always} for higher gate value and E_{never} for lower gate value. Second, the photocurrent through the SPAD should not exceed a certain level, which depends on the difference between the high and low gate voltage levels set by Bob. The explanation of this phenomenon is as follows.

When the SPAD is blinded, a significant current passes through the avalanche photodiode (APD) and the avalanche quenching resistor R_{bias} . The resulting voltage drop across R_{bias} causes a substantial decrease in the APD's supply voltage, consequently shifting its operation mode to one where the avalanche multiplication factor (M) exhibits a linear dependence on the supply voltage (Figure 2) [34].

Thus, when the bias voltage V_{bias} is decreased by ΔV , the current through the $R_{bias} - R_{SPAD}$ circuit drops by:

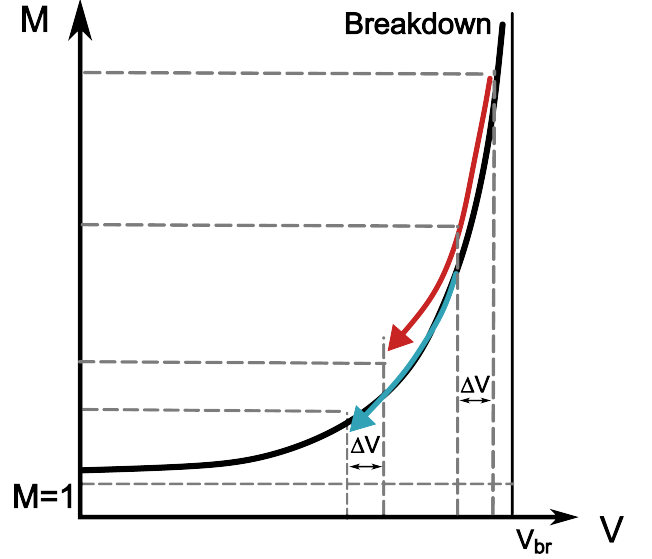


FIG. 2. Avalanche multiplication factor (M) versus APD's supply voltage (V). Blue arrow, red arrow, and dashed lines illustrate the change in M difference between states determined by the default-set supply voltage levels and those under DBA

$$\Delta I \approx \frac{\Delta V}{R_{bias} + R_{SPAD}} \quad (2)$$

Here we assume that $R_{bias} \gg R_0$ and $R_{SPAD} \gg R_0$. Therefore, the voltage drop on the SPAD is:

$$\Delta V_{biasSPAD} \approx \frac{\Delta V R_{SPAD}}{R_{bias} + R_{SPAD}} \quad (3)$$

At the same time when the gate voltage V_{gate} is decreased by ΔV , the SPAD's supply voltage is also decreased by ΔV . Taking into account that $R_{bias} \gg R_{SPAD}$ we get:

$$\Delta V \gg \Delta V_{biasSPAD} \quad (4)$$

The expressions (3) and (4) along with Figure 2 yield several key conclusions. First, the operational mode in case of decreasing bias voltage remains almost the same as the original one. Therefore, the shifted E_{always} and E_{never} energy levels are also close to the ones before the bias level change. Second, varying the gate voltage level appears to be a significantly more effective method for increasing the divergence between operational modes and thus the difference between E_{always}^{high} and E_{never}^{low} . Moreover, the rapid decrease in the gain factor implies that even a small change (1-2 V) in the SPAD's supply voltage substantially increases the energy difference of trigger pulses for high and low gate levels. And finally, if Eve increases blinding radiation energy beyond a certain threshold, the SPAD shifts to the modes with $M \rightarrow 1$. In this regime, the difference between the trigger pulse energy levels will diminish due to the minimal variation in the SPAD's M -factor between the two operational modes.

III. EXPERIMENTAL SETUP

The experimental setup is shown in Figure 3. For our tests, we used a commercially available single-photon detector based on InGaAs/InP APD. Custom-designed electronic circuit enabled precise changing of both bias and gate voltage. The blinding and trigger lasers (BLD LASER and TRIG LASER on the scheme, respectively) are semiconductor laser sources with a 1550 nm wavelength. The first one can operate in both continuous and pulsed regimes and performs switching SPAD from Geiger to linear detection mode. The second one served dual purposes: as a reference light source for the measurement of detection probabilities and for triggering the SPAD in the blinded state. The laser power is controlled using variable optical attenuators (VOA). Coarse wavelength division multiplexer (CWDM) was implemented to mitigate amplified spontaneous emission (ASE) from the laser sources. The required clock signals, their delays and frequencies are set by the Signal generator independently for both laser sources. A 10 MHz reference clock, derived from the signal generator, was distributed to the SPAD under test, an oscilloscope (OSC), and a field-programmable gate array (FPGA) via a time correlator. The oscilloscope was utilized for real-time monitoring of the SPAD's avalanche signals. Statistical analysis of click events was performed by the FPGA.

IV. RESULTS AND DISCUSSION

In this section, we demonstrate the experimental results proving the proposals regarding the difference between E_{always}^{high} and E_{never}^{low} . We also compare the difference between these energy levels under different types of DBA and blinding pulse frequencies.

Thus, we have conducted measurements of the detection probabilities under both pulsed (Figure 4a) and CW (Figure 4b) DBA for identical sets of gate and bias voltages. The pulsed DBA case measurements were also performed across several blinding pulse frequencies, ranging from 2 to 10 MHz, to test the detection system's response to different mean and peak blinding energies. Furthermore, we carried out multiple series of experiments to measure detection probabilities of SPAD in Geiger mode under various supply voltages, achieved by adjusting either gate or bias voltage values. The results are presented in the Table I (default voltage settings: bias = 60.51 V, gate = 3.95 V). As evident from the table, lowering the bias voltage value proved to be even more effective in reducing detection probability than varying the gate voltage.

We first consider the CW DBA case (Figure 4b). When the bias voltage is changed, the ranges $[E_{never}, E_{always}]$ for lower bias voltage and default operational modes overlap almost completely. Conversely, the variations in gate voltage result in minimal or no overlap between these energy ranges. This well-known result allows Eve to impose

TABLE I. Detection probabilities according to supply voltage

Supply voltage	default settings	Bias : 59.82V	Bias : 59.18V	Strobe : 2.81V	Strobe : 2.65V	Strobe : 2.31V
P_{det}^*	10.1	6.45	2.35	6.58	6.45	6.12

* detection probability

bits without leaving any "fingerprints" [29]. The difference in the gap increase between E_{never}^{low} and E_{always}^{high} for the gate level variation approach is insufficient to cause error or double-clicks when the higher trigger pulse is applied, and the default supply voltage is set.

However, when the gate voltage level is changed under the pulsed DBA, the trigger pulse energy level should be increased by more than 25 dB (Figure 4a) to impose a click. At the same time, the change of bias voltage set does not result in any increase between ranges $[E_{never}, E_{always}]$ for default and modified supply voltage sufficient to make an eavesdropper detectable (the condition (1) is not met).

Thus, our proposals in Sec.II are justified. Despite the detection probabilities under normal QKD system operational mode appeared to be almost equal between the gate and bias variation approaches, $\frac{(E_{never}^{low} - E_{always}^{high})}{E_{always}^{high}} \geq 500$ for the gate variation approach whilst there is an overlap in bias-voltage-variation case under the pulsed DBA. Therefore, if Eve tried to impose a click for the lower gate when a higher one is applied, it would inevitably cause error-click (for 1 SPAD-based QKD systems) or double-click events (for 2 SPAD-based QKD systems) when Eve's and Bob's bases do not match. And the probability of such "fingerprints" is rigidly linked to the probability of the successful imposition. This fact allows us to estimate the proportion of total bits attacked solely by estimating the number of "fingerprints" left by Eve, which will be demonstrated in the next section.

Moreover, the gap between E_{always}^{high} and E_{never}^{low} is correlated with the average blinding power (and, therefore, photocurrent) we applied during our test to switch the detectors to the linear mode. The gap keeps increasing with the rise of blinding pulse frequency (see Figure 5) as the corresponding average blinding power level goes down. The positive values of $E_{never}^{low} - 2E_{always}^{default}$ represent cases when the condition (1) is fulfilled. $E_{always}^{default}$ for the given blinding pulses repetition rates represents E_{always} for the default gate level set for underlining the huge gap difference for CW and pulsed DBA. Hence, Eve inevitably causes double- and error-click events and can easily be detected under pulsed DBA, but its presence remains concealed under CW DBA.

On the contrary, CW DBA almost negates the effect due to significant photocurrent increase through APD (applied optical radiation and SPAD's gate overlap). This leads to a decrease in the M-factor, as detailed in Sec.II. Consequently, the system with the countermea-

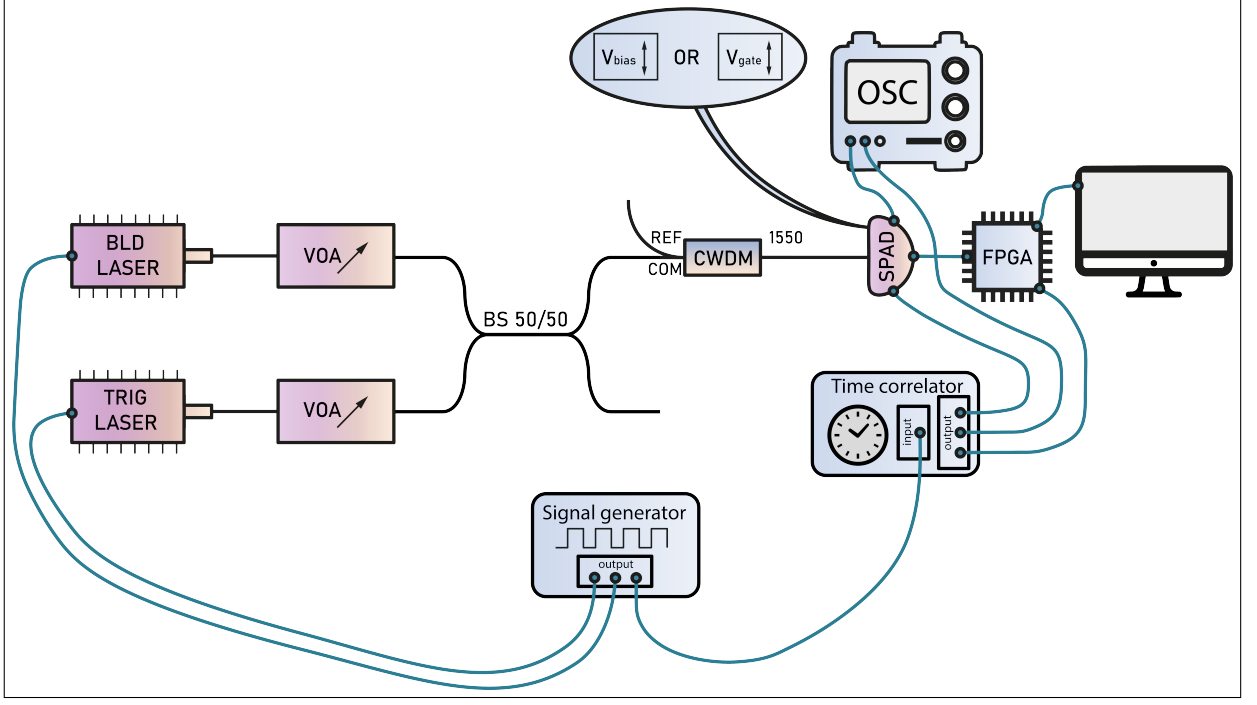


FIG. 3. Experimental setup

sure applied still necessitates support of some basic detector current control [21]. Furthermore, the alarm threshold for the current monitoring system must be carefully calibrated to prevent inevitable fluctuations in the APD's circuit temperature and supply voltage from breaking (1). While the experiment showed an approximate difference of 25 dB between E_{never}^{low} and $2E_{always}^{default}$, random reductions in the supply voltage still decrease the secret key rate. Therefore, maintaining the supply voltage as close as possible to the standard operating level is desirable. Nevertheless, inequality (1) imposes constraints on the permissible range of supply voltage sets.

V. ESTIMATION OF THE SECURE BITS FRACTION

In this section, we provide assessments of the information fraction leaked to the eavesdropper for two and one (see Appendix B) SPAD-based QKD systems.

As we have already claimed, the countermeasure based on the variation of gate voltage levels also allows for assessing the number of imposed clicks. Let Bob randomly choose high or low gate voltage levels (detection efficiencies in Geiger mode are η_1 and η_2) for both detectors simultaneously, with probabilities α and $1 - \alpha$, respectively. If conducting the detector blinding attack on the system with random detectors' efficiency variation, Eve tries to guess not only the basis but also the gate level set by Bob. The adversary sends a trigger pulse with an always-triggering energy level corresponding to the gate voltage level chosen. The probabilities of sending the

E_{always} pulse for a low gate voltage level (higher energy trigger pulse) and the E_{always} pulse for a high gate voltage level (lower energy trigger pulse) are P_{high} and P_{low} , respectively. To set the upper bound of influenced bits, we assume that Eve conducts a fake-state attack on every bit intercepted from Alice. Thus, let's denote $P_{high} = \beta$ and $P_{low} = 1 - \beta$.

Evaluating the number of clicks imposed by an eavesdropper on 2-SPAD-based QKD systems involves several steps. First, Alice and Bob perform the basis reconciliation procedure according to the selected QKD protocol. Second, Bob calculates the number of double-clicks N_{double}^{exp} experimentally observed during the QKD session (or error-clicks N_{error}^{exp} for 1 SPAD-based QKD systems (see Appendix B)). We also assume that all double-click events represent failed imposition attempts. Finally, the determined fraction of double-clicks is compared with the fraction of successfully imposed clicks under DBA to obtain such assessments.

Given a 0.5 probability of basis mismatch between Alice and Eve, approximately half of Eve's imposition attempts are discarded during key sifting. Thus, the experimentally determined fraction of double clicks ($N_{double}^{exp}/N_{sent}$) represents only half of the "fingerprints" left by Eve. Therefore, according to the experimental results obtained in the previous section and assuming the detectors are identical, the double clicks' imposition probability to the total number of fake-states sent by Eve N_{sent} can be assessed as:

$$P_{double}^{bld} = 2 \frac{N_{double}^{exp}}{N_{sent}} = \frac{\alpha\beta}{2} \quad (5)$$

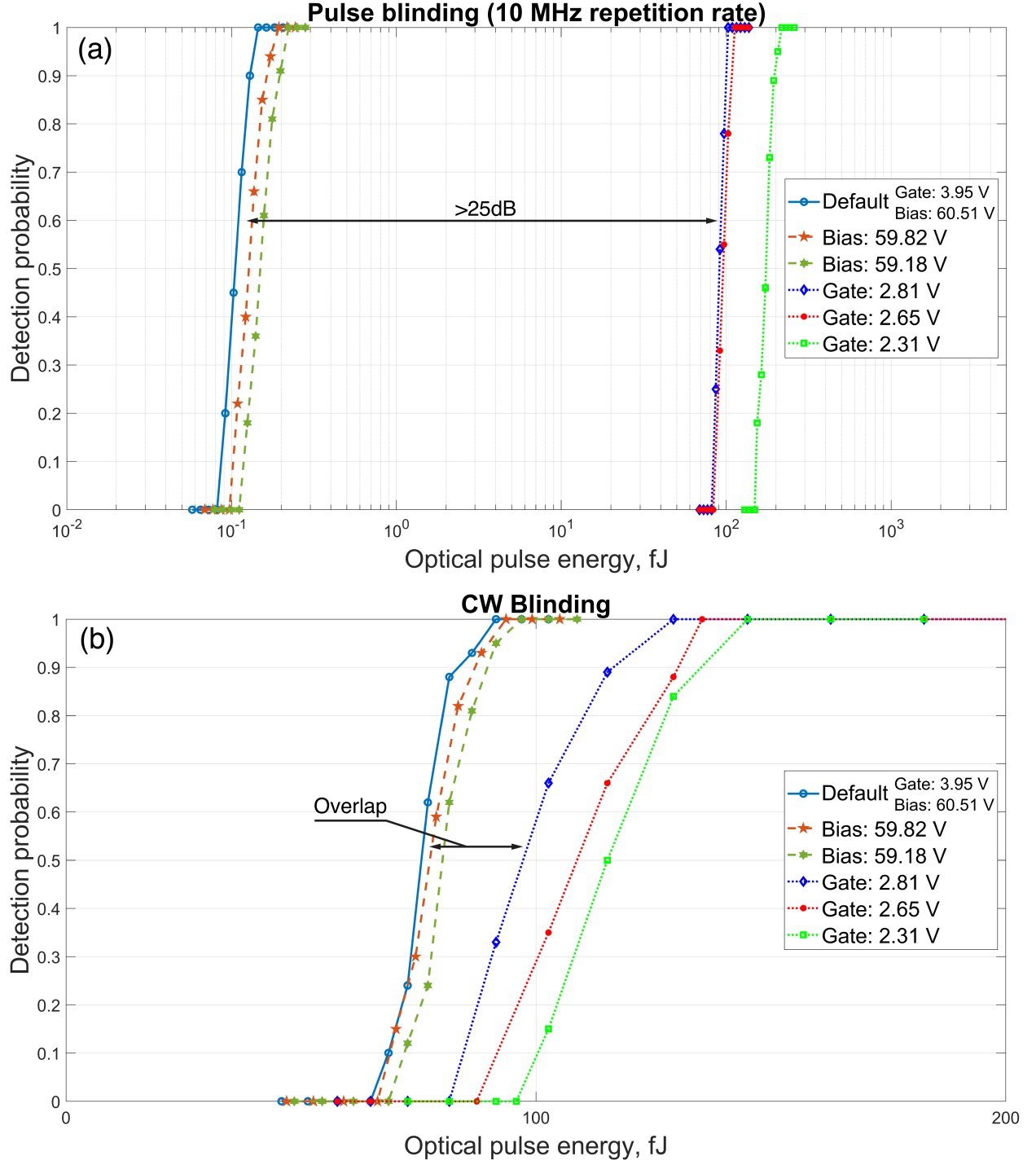


FIG. 4. Detection probabilities versus trigger pulse energies under (a) 10 MHz pulsed blinding and (b) CW blinding

Also, the probability of successfully imposing a click can be represented by the following expression:

$$P_{2SPAD}^{success} = \frac{N_{success}}{N_{sent}} = \frac{\alpha + \beta - \alpha\beta}{2} \quad (6)$$

The detailed derivation of (5) and (6) is provided in Appendix A. Here we denote the assessed number of

successfully imposed Bob's SPADs clicks as $N_{success}$.

The assessed number of fake-states sent by Eve and successfully detected by Bob ($N_{clicked}^{Eve}$) corresponding to the observed number of double clicks is calculated from (5) and (6) as follows:

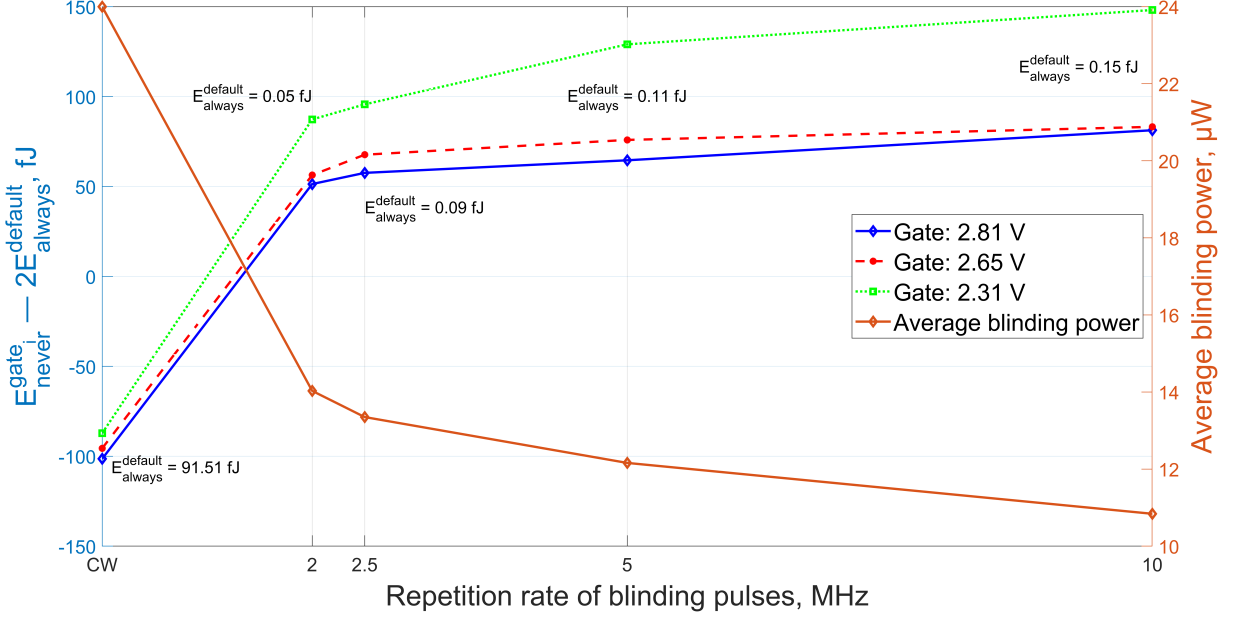


FIG. 5. Testing the condition for leaving "fingerprints" under pulsed (for several blinding pulses repetition rates) and CW DBA. We compare the default-gate-applied (3.95V) case and several lower ones. The average blinding power versus the repetition rate curve indicates correlations between the blinding power and the trigger-pulses energy gap.

$$N_{clicked}^{Eve} = N_{success} + 2N_{double}^{exp} = \frac{1}{2}(\alpha N_{sent} + \frac{4N_{double}^{exp}}{\alpha}) \quad (7)$$

Finally, we calculate the number of experimentally observed clicks on the legitimate user's side ($N_{clicked}^{exp}$) and obtain the following expression for the number of bits that were not attacked by Eve ($N_{key} = N_{clicked}^{exp} - N_{clicked}^{Eve}$):

$$N_{key} = N_{clicked}^{exp} - \frac{1}{2}(\alpha N_{sent} + \frac{4N_{double}^{exp}}{\alpha}) \quad (8)$$

Note that N_{sent} represents the maximum number of bits Eve can send to Bob. Therefore, $N_{sent} = N_{Alice}Q^{Eve}$, where N_{Alice} is the total number of pulses sent by Alice to the quantum channel, Q^{Eve} - Eve's gain for $\{\mu_0, \mu_1, \mu_2\}$ decoy-state protocol [35]:

$$Q^{Eve} = \sum_{i=0}^2 n_i(1 - e^{-\mu_i}) \quad (9)$$

where n_i is the probability of Alice preparing each type of state (decoy or legitimate). For a conservative security analysis, we assume Eve can replace the quantum channel with an ideal channel exhibiting no transmission losses and achieve perfect detection of Alice's signals ($p = 1$), thus increasing the number of states sent to Bob.

We proceed to evaluate the optimal α value for efficient key generation while minimizing Eve's knowledge of

the distributed key under the DBA. The observed during QKD session values $N_{clicked}^{exp}$ and N_{double}^{exp} are perceived as values out of "black box", because the clicks caused by Eve's trigger pulses are indistinguishable from the ones produced by legitimate states. The maximum of (8) is achieved for:

$$\alpha = 2\sqrt{\frac{N_{double}^{exp}}{N_{Alice}Q^{Eve}}} \quad (10)$$

and reaches:

$$N_{key} = N_{clicked}^{exp} - 2\sqrt{N_{double}^{exp}N_{Alice}Q^{Eve}} \quad (11)$$

Given the intrinsic difficulty in distinguishing occasional double-click events occurring during normal QKD system operation from those induced by an eavesdropper conducting DBA, the presented countermeasure should be applied continuously. Therefore, it is essential to ensure that this countermeasure does not substantially decrease the secret key rate when the system operates without an eavesdropper or when an eavesdropper successfully mimics the standard click and double-click rates of Bob's detectors.

For further numerical simulation of the fraction of sifted secure bits after bases reconciliation procedure $S_{key} = N_{key}/N_{clicked}^{exp}$ we consider: $\{0.6, 0.2, 0\}$ decoy-state BB84 protocol, with decoy-states preparation probabilities $n_i = \{0.5, 0.25, 0.25\}$ respectively, the detection efficiency for higher gate $\eta_1 = 0.12$, dark count rate $Y_0 = 10^{-5}$, transmission losses $\eta_{ch} = 10^{-0.02L}$ (L - chan-

nel length). Moreover, we assume that Eve can successfully fake the normal single, error and double-click rates by applying trigger pulses of different E_{always} energies, as well as by letting several pulses pass from Alice to Bob. Therefore, $N_{clicked}^{exp}$ can be expressed as:

$$N_{clicked}^{exp} = Q^{pass} N_{Alice} \quad (12)$$

Q^{pass} - Bob's gain for 2 detectors under normal conditions when legitimate users' bases match:

$$Q^{pass} = \frac{1}{2} \left(\alpha \sum_{i=0}^2 n_i Q_{\eta_1}^{\mu_i} + (1 - \alpha) \sum_{i=0}^2 n_i Q_{\eta_2}^{\mu_i} \right) \quad (13)$$

where $Q_{\eta_j}^{\mu_i} = 1 - (1 - Y_0)e^{-\mu_i \eta_{ch} \eta_j}$ - Bob's gain under normal operation conditions for the given μ_i and η_j .

When no DBA is conducted, the observed double-click gain Q^{double} after bases reconciliation procedure is associated with dark counts and optical system's misalignment $1 - T = 0.01$:

$$Q^{double} = \frac{1}{2} \left(\alpha \sum_{i=0}^2 n_i Q_{\eta_1}^{\mu_i(1-T)} Q_{\eta_1}^{\mu_i T} + (1 - \alpha) \sum_{i=0}^2 n_i Q_{\eta_2}^{\mu_i(1-T)} Q_{\eta_2}^{\mu_i T} \right) \quad (14)$$

Thus, considering that $N_{double}^{exp} = Q^{double} N_{Alice}$, the simulation of the assessed fraction of unaffected bits for various η_2 is presented in Figure (6)

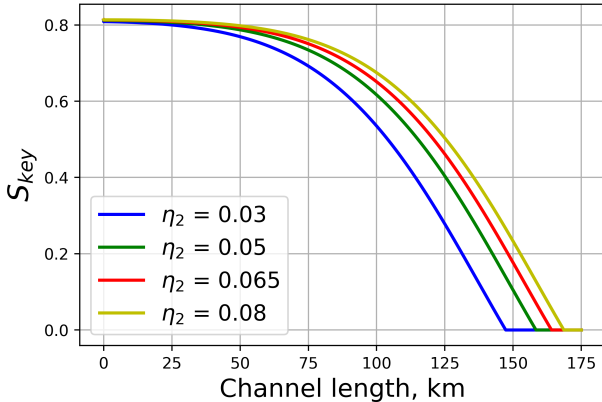


FIG. 6. Secure bit fraction versus QKD channel length for various detection efficiencies (η_2) for a 2-SPAD QKD system under DBA assuming Eve simulates total and double click gains

Thus, we have shown that even if a potential eavesdropper exploits the maximum double-click gain achievable under normal conditions to maximize click imposition attempts during low gates, Bob can select an α value that preserves over half of the default secret key rate after privacy amplification for typical QKD channel lengths

(100-120 km). Moreover, the represented approach allows for secret key generation even under pulsed DBA conducted and successfully detected (e.g., when the normal double-click rate for the high gate is exceeded) due to the ability to assess the fraction of attacked bits and remove them during the privacy amplification procedure.

We also emphasize that the evaluated β parameter determining the fraction of bits exposed to DBA should be calculated considering the finite length of the distributed key. However, it is easy to see, that β -value asymptotically approaches a normal distribution with a mean of $\sim N_{double}^{exp}/N_{sent}$ (5), because the N_{double}^{exp} has a binomial distribution that turns into a normal distribution for large numbers. Therefore, standard deviation of β $\sigma_\beta \sim 1/\sqrt{N_{sent}}$. Therefore, accounting for statistical fluctuations barely impacts the estimated fraction of unblinded bits.

VI. CONCLUSIONS

This study presents both a theoretical framework and empirical evidence demonstrating the efficacy of a countermeasure against DBA. The proposed method leverages statistical analysis of accumulated error and double-click events observed during a QKD session under randomized modulation of SPADs' detection efficiencies via gate voltage manipulation.

We tested random bias and gate-voltage-level variations as countermeasures against click-imposition attacks under pulsed and CW DBA. While CW DBA results aligned with previous findings, new tests of countermeasures against pulsed DBA with a wide range of repetition rates have demonstrated a significant increase in the gap between E_{never}^{low} and E_{always}^{high} compared to the CW DBA scenario. This widening of the energy gap correlates with a reduction in the average blinding power applied during the pulsed DBA. Indeed, the gap between E_{never}^{low} and E_{always}^{high} increased up to ~ 25 dB when the gate voltage was adjusted. Notably, changing the gate voltage proved to be the only effective method for increasing E_{always} by ~ 25 dB while maintaining a non-zero detection efficiency for unblinded detectors.

The required condition $\frac{1}{2} E_{never}^{low} > E_{always}^{high}$ for an eavesdropper leaving "fingerprints" (double- and error-clicks) when attacking low gates is satisfied by a large margin. Thus, we have assessed the fraction of bits affected by Eve for one- and two-SPAD-based QKD systems. This approach firstly limits the amount of information Eve can obtain while being undetected, and secondly allows secret key distribution even under pulsed DBA.

Furthermore, we evaluated the applicability of the proposed countermeasure against pulsed DBA via random variation detectors' gate voltage values for different sets of detection probabilities and optical system imperfections inherent to practical QKD systems. The importance of the represented results lies in providing a se-

cure countermeasure against pulsed DBA while minimally limiting the secret key generation rate. Thus, we conducted numerical simulations of secure key fraction for the QKD system with detectors operating under the supply voltage values close to those utilized in our gap-increase-phenomenon investigations. The simulation results demonstrate that Eve cannot steal more than $\sim 1/3$ of the distributed key without her presence being detected for a 100 km 2-SPAD-based QKD system. However, single-SPAD-based QKD systems require lower dark count rates and better alignment of optical components to achieve similar secure key generation rates.

ACKNOWLEDGEMENTS

The authors gratefully acknowledge the fruitful discussions with S.N. Molotkov and R.Y. Lohmatov.

Appendix A: The derivation of double and successfully-imposed clicks probability

Here, we provide explicit derivation of the (5) and (6). Taking into account the experimental results obtained in Sec.IV, the conditional detection probabilities of causing Bob's detector click are as follows:

$$\begin{aligned} P_{\eta_1}^f | P_{high} &= P_{\eta_2}^f | P_{high} = P_{\eta_1}^h | P_{high} = P_{\eta_1}^f | P_{low} = 1, \\ P_{\eta_2}^h | P_{high} &= P_{\eta_2}^f | P_{low} = P_{\eta_1}^h | P_{low} = P_{\eta_2}^h | P_{low} = 0 \end{aligned} \quad (A1)$$

In (A1), the following designations were used:

$P_{\eta_1}^f | P_{high}$ ($P_{\eta_2}^f | P_{high}$) - the conditional detection probability given a high-power trigger pulse applied during a high (low) gate, under the condition that Eve's and Bob's bases are matched;

$P_{\eta_1}^h | P_{high}$ ($P_{\eta_2}^h | P_{high}$) - the conditional detection probability given a high-power trigger pulse applied during a high (low) gate, under the condition that Eve's and Bob's bases are mismatched;

$P_{\eta_1}^f | P_{low}$ ($P_{\eta_2}^f | P_{low}$) - the conditional detection probability given a low-power trigger pulse applied during a high (low) gate, under the condition that Eve's and Bob's bases are matched;

$P_{\eta_1}^h | P_{low}$ ($P_{\eta_2}^h | P_{low}$) - the conditional detection probability given a low-power trigger pulse applied during a high (low) gate, under the condition that Eve's and Bob's bases are mismatched.

Hence, the probability of causing a double-click event on each pulse sent by Eve is:

$$\begin{aligned} P_{double}^{bld} &= \frac{1}{2} \left(\alpha P_{high} \times P_{\eta_1}^h | P_{high}^2 + \right. \\ &\quad \alpha P_{low} \times P_{\eta_1}^h | P_{low}^2 + \\ &\quad (1 - \alpha) P_{high} \times P_{\eta_2}^h | P_{high}^2 + \\ &\quad \left. (1 - \alpha) P_{low} \times P_{\eta_2}^h | P_{low}^2 \right) \end{aligned} \quad (A2)$$

Therefore, according to (A1) and (A2), the double clicks' imposition probability to the total number of fake-states sent by Eve N_{sent} can be assessed:

$$P_{double}^{bld} = \frac{\alpha\beta}{2} \quad (A3)$$

Similarly, according to (A1) and assuming the detectors are identical, the probability to successfully impose a click can be represented by the following expression:

$$\begin{aligned} P_{2SPAD}^{success} &= \frac{1}{2} \left(\alpha P_{high} \times (P_{\eta_1}^f | P_{high} + P_{\eta_1}^h | P_{high} - P_{\eta_1}^h | P_{high}^2) + \right. \\ &\quad \alpha P_{low} \times (P_{\eta_1}^f | P_{low} + P_{\eta_1}^h | P_{low} - P_{\eta_1}^h | P_{low}^2) + \\ &\quad (1 - \alpha) P_{high} \times (P_{\eta_2}^f | P_{high} + P_{\eta_2}^h | P_{high} - P_{\eta_2}^h | P_{high}^2) + \\ &\quad \left. (1 - \alpha) P_{low} \times (P_{\eta_2}^f | P_{low} + P_{\eta_2}^h | P_{low} - P_{\eta_2}^h | P_{low}^2) \right) = \\ &= \frac{\alpha + \beta - \alpha\beta}{2} \end{aligned} \quad (A4)$$

Appendix B: Estimation of the secure bits fraction for one-SPAD-based QKD

Likewise to the two-SPAD-based approach, we first determine the probability of causing an error per trigger pulse sent by Eve under DBA for a 1 SPAD-based QKD system based on the estimated number of errors after the bases reconciliation procedure (N_{error}^{exp}):

$$\begin{aligned} P_{1SPAD}^{error} &= \frac{1}{4} \left(\alpha P_{high} P_{\eta_1}^h | P_{high} + (1 - \alpha) P_{high} P_{\eta_2}^h | P_{high} + \right. \\ &\quad \left. \alpha P_{low} P_{\eta_1}^h | P_{low} + (1 - \alpha) P_{low} P_{\eta_2}^h | P_{low} \right) = \\ &= \frac{\alpha\beta}{4} = 1/2 P_{double}^{bld} = \frac{2N_{error}^{exp}}{N_{sent}} \end{aligned} \quad (B1)$$

Secondly, in the case of a QKD system employing a single detector, the probability of successful click imposition can be expressed as:

$$\begin{aligned}
P_{1SPAD}^{succ} &= \frac{1}{4} \left(\alpha P_{high} \times (P_{\eta_1}^f | P_{high} + P_{\eta_1}^h | P_{high}) + \right. \\
&\quad \alpha P_{low} \times (P_{\eta_1}^f | P_{low} + P_{\eta_1}^h | P_{low}) + \\
&\quad (1 - \alpha) P_{high} \times (P_{\eta_2}^f | P_{high} + P_{\eta_2}^h | P_{high}) + \\
&\quad \left. (1 - \alpha) P_{low} \times (P_{\eta_2}^f | P_{low} + P_{\eta_2}^h | P_{low}) \right) = \\
&= \frac{\alpha + \beta}{4} = \frac{N_{success}^{one}}{N_{sent}} \quad (B2)
\end{aligned}$$

From (B1) we can also estimate the fraction of strong pulses sent by Eve corresponding to N_{error}^{exp} :

$$\beta = \frac{8N_{error}^{exp}}{\alpha N_{sent}} \quad (B3)$$

The number of successfully imposed bits $N_{success}^{one}$ obtained from (B2) and (B3) is:

$$N_{success}^{one} = \frac{\alpha N_{sent}}{4} + \frac{2N_{error}^{exp}}{\alpha} \quad (B4)$$

Hence, the total number of clicks unexposed to Eve fake-state attack, can be evaluated as:

$$N_{key}^{one} = N_{clicked}^{exp} - \frac{\alpha N_{sent}}{4} - \frac{2N_{error}^{exp}(1 + \alpha)}{\alpha} \quad (B5)$$

For numerical simulations of the unblinded key fraction in a single-SPAD receiver QKD system, we substitute Q^{pass} with $1/2 Q^{pass}$ in (12), reflecting that Bob successfully registers only half the bits. To highlight the negative influence of receiver optical misalignment, we consider considerably higher extinction ratios than for 2-SPAD systems. We also assume Eve introduces a typical quantum bit error rate (QBER).

QBER is determined by optical system misalignment and dark count rate set by the following expression:

$$\begin{aligned}
QBER &= \frac{1}{2} \left(\alpha \sum_{i=0}^2 n_i Q_{\eta_1}^{\mu_i(1-T)} + \right. \\
&\quad \left. (1 - \alpha) \sum_{i=0}^2 n_i Q_{\eta_2}^{\mu_i(1-T)} \right) \quad (B6)
\end{aligned}$$

Thus,

$$N_{error}^{exp} = QBER * N_{Alice} \quad (B7)$$

Following a similar approach outlined in Sec.V, we treat N_{error}^{exp} as "black-box" parameter. Consequently,

the optimal α value for minimizing the estimated number of bits accessible to Eve under DBA is:

$$\alpha = 2 \sqrt{\frac{2N_{error}^{exp}}{N_{Alice} Q^{Eve}}} \quad (B8)$$

Therefore, the minimal number of bits influenced by Eve N_{one}^{Eve} corresponding to α from (B5) is represented by the following expression:

$$N_{one}^{Eve} = \sqrt{2N_{error}^{exp} N_{Alice} Q^{Eve}} + 2N_{error}^{exp} \quad (B9)$$

Figure 7 shows the simulated unaffected key fraction (S_{key}^{1SPAD}) for $\eta_2 = 0.8$ and various optical system misalignment values (1-T).

Comparing the estimated number of legitimate bits for one- and two-SPAD-based QKD systems reveals that imperfections in the receiver's optical and detection systems have a significantly more pronounced impact on single-SPAD systems than on their two-SPAD counterparts. This stems from the much lower intrinsic rate of double-click events compared to errors. Thus, being unable to distinguish error clicks caused by Eve from those arising due to system misalignment and dark counts, we regard all these events as the violator's influence. Therefore, single-SPAD systems require a reduction in dark count and extinction rates by several orders of magnitude to achieve comparable performance.

Nevertheless, similar to the 2-SPAD-based QKD systems, the number of error clicks follows a binomial distribution, approximating a normal distribution for large numbers. Given, that β -value $\sim N_{error}^{exp}/N_{sent}$ (B3), the standard deviation of β $\sigma_\beta \sim 1/\sqrt{N_{sent}}$. Therefore, considering statistical fluctuations will have an insignificant impact on the fraction of legitimate bits.

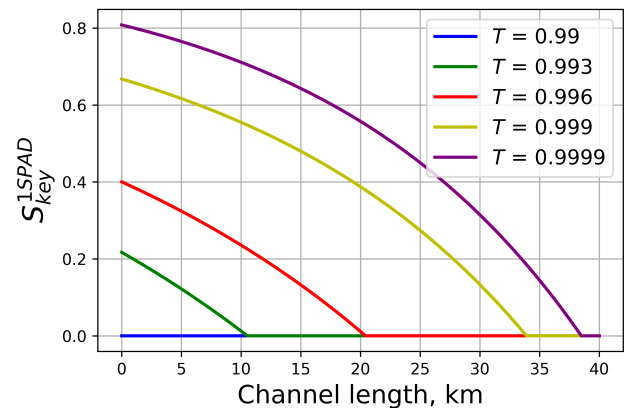


FIG. 7. Secure bit fraction versus QKD channel length for a 1-SPAD QKD system under DBA, for various extinction ratios (T) assuming Eve simulates total and error click gains

-
- [1] W. K. Wootters and W. H. Zurek, A single quantum cannot be cloned, *Nature* **299**, 802 (1982).
 - [2] N. Gisin, S. Fasel, B. Kraus, H. Zbinden, and G. Ribordy, Trojan-horse attacks on quantum-key-distribution systems, *Physical Review A—Atomic, Molecular, and Optical Physics* **73**, 022320 (2006).
 - [3] A. N. Bugge, S. Sauge, A. M. M. Ghazali, J. Skaar, L. Lydersen, and V. Makarov, Laser damage helps the eavesdropper in quantum cryptography, *Physical review letters* **112**, 070503 (2014).
 - [4] S. V. Alferov, K. E. Bugai, and I. A. Pargachev, Study of the vulnerability of neutral optical filters used in quantum key distribution systems against laser damage attack, *JETP Letters* **116**, 123 (2022).
 - [5] L. Lydersen, C. Wiechers, C. Wittmann, D. Elser, J. Skaar, and V. Makarov, Hacking commercial quantum cryptography systems by tailored bright illumination, *Nature photonics* **4**, 686 (2010).
 - [6] S. Sauge, L. Lydersen, A. Anisimov, J. Skaar, and V. Makarov, Controlling an actively-quenched single photon detector with bright light, *Optics Express* **19**, 23590 (2011).
 - [7] A. Huang, Á. Navarrete, S.-H. Sun, P. Chaiwongkhot, M. Curty, and V. Makarov, Laser-seeding attack in quantum key distribution, *Physical Review Applied* **12**, 064043 (2019).
 - [8] C. Wiechers, L. Lydersen, C. Wittmann, D. Elser, J. Skaar, C. Marquardt, V. Makarov, and G. Leuchs, After-gate attack on a quantum cryptosystem, *New Journal of Physics* **13**, 013043 (2011).
 - [9] V. Makarov, A. Anisimov, and J. Skaar, Effects of detector efficiency mismatch on security of quantum cryptosystems, *Physical Review A—Atomic, Molecular, and Optical Physics* **74**, 022313 (2006).
 - [10] B. Qi, C.-H. F. Fung, H.-K. Lo, and X. Ma, Time-shift attack in practical quantum cryptosystems, *arXiv preprint quant-ph/0512080* (2005).
 - [11] L. Lydersen, M. K. Akhlaghi, A. H. Majedi, J. Skaar, and V. Makarov, Controlling a superconducting nanowire single-photon detector using tailored bright illumination, *New Journal of Physics* **13**, 113042 (2011).
 - [12] P. Jouguet, S. Kunz-Jacques, and E. Diamanti, Preventing calibration attacks on the local oscillator in continuous-variable quantum key distribution, *Physical Review A—Atomic, Molecular, and Optical Physics* **87**, 062313 (2013).
 - [13] S. A. Bogdanov, I. S. Sushchev, A. N. Klimov, K. E. Bugai, D. Bulavkin, and D. Dvoretzky, Influence of qkd apparatus parameters on the backflash attack, in *Quantum Technologies 2022*, Vol. 12133 (SPIE, 2022) pp. 90–95.
 - [14] I. S. Sushchev, D. S. Bulavkin, K. E. Bugai, A. S. Sidelnikova, and D. A. Dvoretzkiy, Trojan-horse attack on a real-world quantum key distribution system: Theoretical and experimental security analysis, *Physical Review Applied* **22**, 034032 (2024).
 - [15] K. Bugai, I. Sushchev, D. Bulavkin, R. Y. Lokhmatov, and D. Dvoretzkiy, Protection method against powerful emission attacks based on optical-fiber fuse element, in *2024 International Conference Laser Optics (ICLO)* (IEEE, 2024) pp. 446–446.
 - [16] V. Lovic, D. G. Marangon, P. Smith, R. I. Woodward, and A. J. Shields, Quantified effects of the laser-seeding attack in quantum key distribution, *Physical Review Applied* **20**, 044005 (2023).
 - [17] L. Lydersen, C. Wiechers, C. Wittmann, D. Elser, J. Skaar, and V. Makarov, Thermal blinding of gated detectors in quantum cryptography, *Optics express* **18**, 27938 (2010).
 - [18] V. Makarov, Controlling passively quenched single photon detectors by bright light, *New Journal of Physics* **11**, 065003 (2009).
 - [19] D. Bulavkin, I. Sushchev, K. Bugai, S. Bogdanov, and D. Dvoretzkiy, Study of a single-photon detector blinding attack with modulated bright light, in *Quantum and Nonlinear Optics IX*, Vol. 12323 (SPIE, 2023) pp. 73–78.
 - [20] Z. Wu, A. Huang, H. Chen, S.-H. Sun, J. Ding, X. Qiang, X. Fu, P. Xu, and J. Wu, Hacking single-photon avalanche detectors in quantum key distribution via pulse illumination, *Optics Express* **28**, 25574 (2020).
 - [21] Z. Yuan, J. Dynes, and A. Shields, Resilience of gated avalanche photodiodes against bright illumination attacks in quantum cryptography, *Applied physics letters* **98** (2011).
 - [22] V. Chistiakov, A. Huang, V. Egorov, and V. Makarov, Controlling single-photon detector id210 with bright light, *Optics express* **27**, 32253 (2019).
 - [23] Y.-J. Qian, D.-Y. He, S. Wang, W. Chen, Z.-Q. Yin, G.-C. Guo, and Z.-F. Han, Robust countermeasure against detector control attack in a practical quantum key distribution system, *Optica* **6**, 1178 (2019).
 - [24] Z. Wu, A. Huang, X. Qiang, J. Ding, P. Xu, X. Fu, and J. Wu, Robust countermeasure against detector control attack in a practical quantum key distribution system: comment, *Optica* **7**, 1391 (2020).
 - [25] P. Acheva, K. Zaitsev, V. Zavodilenko, A. Losev, A. Huang, and V. Makarov, Automated verification of countermeasure against detector-control attack in quantum key distribution, *EPJ Quantum Technology* **10**, 22 (2023).
 - [26] L. Shen and C. Kurtsiefer, Countering detector manipulation attacks in quantum communication through detector self-testing, *APL Photonics* **10** (2025).
 - [27] C. C. W. Lim, N. Walenta, M. Legré, N. Gisin, and H. Zbinden, Random variation of detector efficiency: A countermeasure against detector blinding attacks for quantum key distribution, *IEEE Journal of Selected Topics in Quantum Electronics* **21**, 192 (2015).
 - [28] M. Legré and G. Ribordy, Apparatus and method for the detection of attacks taking control of the single photon detectors of a quantum cryptography apparatus by randomly changing their efficiency (2018), *uS Patent* 10,020,937.
 - [29] A. Huang, S. Sajeed, P. Chaiwongkhot, M. Soucarros, M. Legré, and V. Makarov, Testing random-detector-efficiency countermeasure in a commercial system reveals a breakable unrealistic assumption, *IEEE Journal of Quantum Electronics* **52**, 1 (2016).
 - [30] S. Kulik and S. Molotkov, Decoy state method for quantum cryptography based on phase coding into faint laser pulses, *Laser Physics Letters* **14**, 125205 (2017).
 - [31] S. Molotkov, A method for detecting detector blinding

- attacks in quantum cryptography systems with polarization coding (2021), russian Patent 2,783,977.
- [32] F. Bussières and G. Gaëtan, Blinding attack detecting device and method (2020), european Patent 3,716,252.
 - [33] G. Gras, D. Rusca, H. Zbinden, and F. Bussières, Countermeasure against quantum hacking using detection statistics, *Physical Review Applied* **15**, 034052 (2021).
 - [34] S. Cova, M. Ghioni, A. Lacaita, C. Samori, and F. Zappa, Avalanche photodiodes and quenching circuits for single-photon detection, *Applied optics* **35**, 1956 (1996).
 - [35] X. Ma, B. Qi, Y. Zhao, and H.-K. Lo, Practical decoy state for quantum key distribution, *Physical Review A—Atomic, Molecular, and Optical Physics* **72**, 012326 (2005).